Journal of Materials Chemistry

Cite this: J. Mater. Chem., 2012, 22, 5190

www.rsc.org/materials

PAPER

Functionalized cyano-OPVs as melt-processable two-photon absorbers†

Brian T. Makowski,[a] Joseph Lott,[a] Brent Valle,[b] Kenneth D. Singer*[b] and Christoph Weder*[ac]

Received 14th November 2011, Accepted 5th January 2012
DOI: 10.1039/c2jm15846a

Several cyano-functionalized oligo(phenylenevinylene) (cyano-OPV) dyes were modified with different alkyl substituents with the objective to develop melt-processable, two-photon absorbing materials. The new dyes exhibit two-photon absorption cross-sections in the range of 400–850 GM, can be melt-processed at temperatures as low as ~100 °C, and offer high thermal stability. The propensity of these molecules to form excimers also makes them interesting for sensor and data storage applications.

1. Introduction

Two-photon absorption (TPA) is a nonlinear optical (NLO) process that involves the simultaneous absorption of two photons of identical or different frequencies, leading to the excitation of a molecule from the ground state to a higher energy electronic state.[1] TPA-related processes such as nonlinear transmission and intensity-dependent refraction can be exploited in a plethora of optoelectronic devices such as waveguides,[2] optical switches,[3] lasers,[4] optical limiters,[5] and 3-dimensional optical data storage systems.[6] TPA can also be used to trigger subsequent events, such as fluorescence or chemical reactions, which enable applications such as biological imaging,[7] photodynamic therapy,[8] and 3-dimensional lithography.[9] Significant efforts have been directed towards the development of organic TPA chromophores that possess large TPA cross-sections (σ), which permit one to exploit NLO processes with lower-energy light sources. Strategies to maximize a chromophore's σ include extending the conjugation length and dimensionality,[10,11] as well as the introduction of electron donating/accepting (D/A) groups to create "push–pull" systems.[12] An effective design involves symmetrically substituted D–π–D chromophores in which two donors are conjugated by a bridge (π) so that excitation leads to large changes of the quadrupole moment.[13] The integration of additional electron-accepting groups in the conjugated system, so that D–π–A–π–D structures are created, further increases σ.[12]

Maximization of σ, however, often comes at the expense of processability, since extended π-systems usually exhibit high melting and dissolution enthalpies and low melting and dissolution entropies, leading to limited solubility and high melting temperatures. Nevertheless, for many devices, such as optical switches, multiplexers based on macroporous silicon structures that are locally infiltrated with a neat NLO dye,[14] or multilayered adaptive dielectric mirrors,[15] it would be desirable if the NLO material could be melt-processed at low temperatures and/or processed from high-concentration solutions. We here report the investigation of several cyano-substituted oligo(phenylenevinylene)s (cyano-OPVs, Fig. 1), which can offer rather large two-photon absorption cross-sections and are readily melt-processed at temperatures as low as ~100 °C. These properties, together with their propensity to form excimers, render them attractive for use in polymer-based optical storage systems that operate on the basis of TPA-induced switching of the aggregation state and fluorescence.[6]

Many low-molecular weight oligo(phenylene vinylene) dyes (OPVs) have already been reported to display appreciable TPA cross-sections of between 400 and 2000 GM, depending upon the detailed chemical structure and also the solvent.[16,17] The largest nonlinearities are seen in OPVs in which donor and acceptor groups are connected to create D–π–A–π–D structures, with the objective to maximize the extent of intramolecular charge

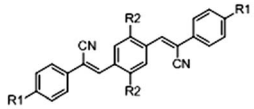

Dye	R1	R2
A1	OMe	OMe
A2	$OC_{18}H_{37}$	OMe
A3	EHO	OMe
A4	EHO	OC_8H_{17}
B1	OMe	H
B2	EHO	H
C1	NO_2	H
C2	NO_2	DMO

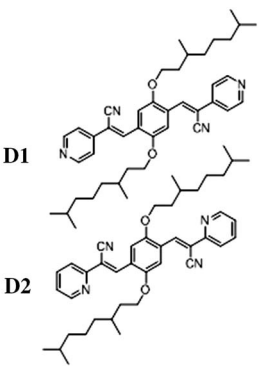

Fig. 1 Chemical structures of the nonlinear optical dyes investigated in this study. EHO = 2-ethylhexyloxy; DMO = 3,7-dimethyloctyloxy.

[a]*Department of Macromolecular Science and Engineering, Case Western Reserve University, Cleveland, OH, 44106, USA*
[b]*Department of Physics, Case Western Reserve University, Cleveland, OH, 44106, USA*
[c]*Adolphe Merkle Institute and Fribourg Center for Nanomaterials, University of Fribourg, CH-1723 Marly 1, Switzerland. E-mail: kenneth.singer@case.edu; christoph.weder@unifr.ch*

† Electronic supplementary information (ESI) available: Crystallographic data and procedures for the structural analysis of **A3**; differential scanning calorimetry traces; absorbance and fluorescence spectra. See DOI: 10.1039/c2jm15846a

transfer (ICT). For example, Pond *et al.* showed that the attachment of cyano groups to the central benzene ring in OPVs with peripheral donor groups increases σ by as much as 900 GM.[18] Interestingly, the TPA response of OPVs featuring cyano groups attached to the vinylene bridge, and which may be viewed as compact D–π–A–π–D–π–A–π–D systems, has been little explored. The compounds found in the literature all carry the cyano groups in the vinylene positions close to the central benzene ring (CN′-OPVs).[19] With respect to maximizing σ, this configuration is not ideal, since cyano groups in this position are known to twist the molecule out of plane,[19] thereby limiting conjugation and ICT.[20] By contrast, the placement of cyano groups on the vinylene position away from the central ring (CN″-OPVs) results in planar molecules.[19] Such CN″-OPVs have attracted our attention as fluorescent "chameleon dyes" due to their propensity to form highly fluorescent excimer complexes and the ability to change their emission color upon (dis) assembly.[21] In this context, the high stability of these molecules has been exploited to melt-process them either in their neat form or as blends with a range of different polymers.[21] Nonetheless, the TPA of such CN″-OPVs has received little attention, perhaps on account of the comparably low TPA properties of CN′-OPVs. Departing from one CN″-OPV derivative whose TPA cross-section was recently reported (Fig. 1, **A2**), we here explore systematic structural variations with the objective to maximize σ and minimize the melting temperature (T_m) for optimum processability. All of the new dyes form highly fluorescent excimer complexes and display significant emission color changes upon transition from solution to the solid state, which makes them also interesting for sensor applications[21] and optical data storage schemes.[6]

2. Experimental section

Materials and methods

All commercial reagents were used as received unless otherwise stated in the text. 4-(2-Ethylhexyloxy)phenylacetonitrile,[22] and molecules **A1**,[23] **A2**,[24] **A3**,[22] and **B1**[23] were prepared as previously described. ^{1}H NMR spectra were recorded on Varian 300 MHz and 600 MHz NMR spectrometers. Chemical shifts were expressed in ppm relative to the internal chloroform peak at 7.26 ppm. Elemental analyses were conducted by Galbraith Laboratories, Inc.

Synthesis of (2*Z*,2′*Z*)-3,3′-(2,5-bis(octyloxy)-1,4-phenylene) bis(2-(4-((2-ethylhexyl)oxy)phenyl)acrylonitrile) (A4)

4-(2-Ethylhexyloxy)phenylacetonitrile (156 mg, 0.64 mmol), 2,5-bis(octyloxy)terephthaldehyde (112 mg, 0.29 mmol), THF (4 mL) and *t*-buOH (11 mL) were combined and heated to 50 °C while stirred. *t*-buOK (0.058 mL of a 1 M solution in THF) and Bu_4NOH (0.58 mL of a 1 M solution in methanol) were added quickly and the mixture turned green. The reaction mixture was stirred for another 15 min, cooled to room temperature, and poured into acidified methanol (30 mL containing 1 drop of concentrated acetic acid). The precipitate was filtered off, excessively washed with methanol, and dried *in vacuo* at 50 °C to yield **A4** in the form of an orange powder (151 mg, 60%). ^{1}H NMR ($CDCl_3$): δ = 7.90 (s, 2H), 7.85 (s, 2H), 7.62 (d, 4H), 6.97 (d, 4H), 4.14 (t, 4H), 3.93 (d, 4H), 1.86 (m, 4H), 1.80 (m, 2H), 1.57–1.20 (m, 36H), 0.99 (3t, 18H). Calcd: C, 79.57; H, 9.54; N, 3.31. Found: C, 79.39; H, 9.35; N, 3.43%.

Synthesis of (2*Z*,2′*Z*)-3,3′-(1,4-phenylene)bis(2-(4-((2-ethylhexyl)oxy)phenyl)acrylonitrile) (B2)

4-(2-Ethylhexyloxy)phenylacetonitrile (340 mg, 1.4 mmol), terephthaldehyde (91 mg, 0.68 mmol), THF (5.7 mL) and *t*-buOH (17 mL) were combined and heated to 50 °C while stirred. *t*-buOK (0.136 mL of a 1 M solution in THF) and Bu_4NOH (1.35 mL of a 1 M solution in methanol) were added quickly and a yellow precipitate formed. The reaction mixture was stirred for another 15 min, cooled to room temperature, and poured into acidified methanol (34 mL containing 1 drop of concentrated acetic acid). The precipitate was filtered off, excessively washed with methanol, and dried *in vacuo* at 50 °C to yield **B2** in the form of a red powder (240 mg, 60%). ^{1}H NMR ($CDCl_3$): δ = 7.95 (s, 4H), 7.63 (d, 4H), 7.43 (s, 2H), 6.98 (d, 4H), 3.91 (d, 4H), 1.76 (m, 4H), 1.55–1.30 (m, 16H), 0.88 (2t, 12H). Calcd: C, 81.59; H, 8.22; N, 4.76. Found: C, 81.49; H, 7.85; N, 4.86%.

Synthesis of (2*Z*,2′*Z*)-3,3′-(1,4-phenylene)bis(2-(4-nitrophenyl) acrylonitrile) (C1)

Terephthaldehyde (0.529 g, 4.0 mmol) and 4-nitrophenylacetonitrile (1.376 g, 8.5 mmol) were combined in a 250 mL 3-neck round-bottom flask. Methanol (100 mL) was added and the mixture was stirred at 50 °C until the reactants had dissolved. Piperidine (0.86 mL) was quickly added *via* a syringe. The color of the reaction mixture instantly turned purple and a yellow precipitate formed after ~2 min. The reaction mixture was stirred for another 30 min at 50 °C, cooled to room temperature, and poured into acidified methanol (380 mL containing 8 drops of concentrated acetic acid). The precipitate was filtered off and dried *in vacuo* at 50 °C overnight. Recrystallization from DMF yielded **C1** in the form of an orange powder (1.18 g, 71%). Calcd: C, 68.24; H, 3.34; N, 13.26. Found: C, 67.57; H, 3.35; N, 13.30%.

Synthesis of (2*Z*,2′*Z*)-3,3′-(2,5-bis((3,7-dimethyloctyl)oxy)-1,4-phenylene)bis(2-(4-nitrophenyl)acrylonitrile) (C2)

2,5-Bis(3,7-dimethyloctyloxy)terephthaldehyde (0.200 g, 0.45 mmol) and 4-nitrophenylacetonitrile (0.1597 g, 0.99 mmol) were combined in a 25 mL 3-neck round-bottom flask. THF (2.6 mL) and *t*-buOH (7.8 mL) were added and the mixture was stirred at 60 °C until the reactants had dissolved. Piperidine (0.11 mL) was quickly added *via* a syringe. The color of the reaction mixture instantly turned orange. The reaction mixture was stirred for another 60 min at 60 °C and subsequently cooled to room temperature. The solvents were removed using a rotary evaporator. The remaining solid was dissolved in $CHCl_3$, the solution was filtered through a plug of silica gel, and the solvent was removed using a rotary evaporator. The crude orange product was recrystallized from 2-propanol to yield **C2** in the form of a deep red powder (0.200 g, 60%). ^{1}H NMR ($CDCl_3$): δ = 8.34 (d, 4H), 8.19 (s, 2H), 7.95 (s, 2H), 7.86 (s, 4H), 4.21 (t, 4H), 1.93 (m, 2H), 1.69–1.12 (m, 14H), 0.98 (d, 6H), 0.84 (d, 12H). Calcd: C, 71.91; H, 7.41; N, 7.62. Found: C, 71.49; H, 7.07; N, 7.58%.

Synthesis of (2*Z*,2′*Z*)-3,3′-(2,5-bis(octyloxy)-1,4-phenylene) bis(2-(pyridin-4-yl)acrylonitrile) (D1)

2,5-Bis(3,7-dimethyloctyloxy)-terephthaldehyde (0.150 g, 0.33 mmol) and 4-pyridine acetonitrile hydrochloride (0.115 g, 0.74 mmol) were combined in a 25 mL 3-neck round-bottom flask. THF (2.0 mL) and *t*-buOH (5.9 mL) were added and the mixture was heated to 60 °C, while stirring. H_2O (1.0 mL) was added and the mixture was stirred until the reactants had dissolved. Piperidine (0.07 mL) was quickly added *via* a syringe and the reaction color instantly turned yellow. The reaction mixture was stirred for another 90 min at 60 °C, cooled to room temperature, and poured into acidified methanol (50 mL containing 1 drop of concentrated acetic acid). The precipitate was filtered off and dried *in vacuo* at 50 °C overnight. Recrystallization from boiling methanol to which a few drops of H_2O had been added yielded **D1** in the form of an orange powder (0.978 g, 45%). ^{1}H NMR ($CDCl_3$): $\delta = 8.73$ (d, 4H), 8.25 (s, 2H), 7.95 (s, 2H), 7.58 (d, 4H), 4.20 (t, 4H), 1.93 (m, 2H), 1.72–1.12 (m, 18H), 0.98 (d, 6H), 0.85 (d, 12H). Calcd: C, 77.98, H, 8.41; N, 8.66. Found: C, 77.33; H, 8.22; N, 8.46%.

Synthesis of (2*Z*,2′*Z*)-3,3′-(2,5-bis(octyloxy)-1,4-phenylene) bis(2-(pyridin-2-yl)acrylonitrile) (D2)

2,5-Bis(3,7-dimethyloctyloxy)-terephthaldehyde (0.150 g, 0.33 mmol) and 2-pyridine acetonitrile (0.087 g, 0.88 mmol) were combined in a 25 mL 3-neck round-bottom flask. THF (2.0 mL) and *t*-buOH (5.9 mL) were added and the mixture was stirred at 55 °C until the reactants had dissolved. A solution of Bu_4NOH (3 drops of a 1.0 M solution in methanol) in THF (5.0 mL) was added drop-wise to the reaction mixture over the course of 10 min. The reaction mixture was stirred for another 60 min at 55 °C, cooled to room temperature, and poured into acidified methanol (50 mL containing 1 drop of concentrated acetic acid). The precipitate was filtered off and dried *in vacuo* at 50 °C overnight. Recrystallization from boiling methanol to which a few drops of H_2O had been added yielded **D2** in the form of an orange powder (0.117 g, 54%). ^{1}H NMR ($CDCl_3$): $\delta = 8.87$ (s, 2H), 8.67 (d, 2H), 7.96 (s, 2H), 7.74 (m, 4H), 7.30 (m, 2H), 4.20 (t, 4H), 1.92 (m, 2H), 1.76–1.11 (m, 18H), 0.97 (d, 6H), 0.84 (d, 12H). Calcd: C, 77.98; H, 8.41; N, 8.66. Found: C, 77.27; H, 8.16; N, 8.67%.

Differential scanning calorimetry

The differential scanning calorimetry (DSC) traces were recorded using a Mettler-Toledo DSC-1 equipped with a Huber TC-100 cooling regulation system. All traces were recorded in a nitrogen atmosphere with heating and cooling rates of 10 K min^{-1}, except for dye **A3**, which was recorded at a rate of 5 K min^{-1}.

UV-Vis spectroscopy

UV-Vis absorbance spectra were recorded in chloroform (>99.8% containing 0.75% ethanol as stabilizer) on a Perkin Elmer Instruments Lambda 800 UV-VIS spectrophotometer. For quantum yield measurements, absorbances were measured on a CARY 500 UV-VIS-NIR spectrophotometer.

Steady-state photoluminescence spectroscopy

All photoluminescence (PL) measurements were acquired using a Photon Technology International QuantaMaster 40 spectrophotometer under excitation at the wavelength of maximum absorption; the spectra were corrected for instrument throughput and detector response. Quantum yields in degassed toluene ($n = 1.497$) were determined according to the general protocol given in ref. 34 using Rhodamine 6G in EtOH ($n = 1.361$) as reference. Experiments were conducted with samples that had an absorbance of 0.05–0.1 in a 1 cm cuvette on a Horiba Fluorolog 3 with Xenon arc lamp source.

Determination of solubility in chloroform

The solubility was determined by weighing a known amount of the respective dye and adding chloroform in small increments while periodically sonicating the solution until the dye appeared to be visually dissolved. Since these dyes tend to form excimers and therefore should emit light at longer wavelengths when not fully dissolved, the solutions were also observed under 365 nm UV-light.

Two-photon absorption measurements

Two photon absorption spectra were measured at wavelengths between 625 and 725 nm using the open-aperture Z-scan technique.[25] A Ti:Sapphire regenerative amplifier (CPA-2010, from Clark-MXR) with 200 fs pulse duration and 1 mJ pulse energy pumped a traveling-wave optical parametric amplifier of superfluorescence (TOPAS, Light Conversion Ltd.). The second harmonic of the signal was passed through a spatial filter to isolate the lowest-order transverse mode of the beam. The beam was then split into a signal and reference arm which was used to divide by shot-to-shot noise. The beam waist and confocal parameter were determined through measurements of the beam size using a rotating slit beam profiler (BP104-VIS, Thorlabs Inc.) at several *z*-positions and then fitting these points to the well-known Gaussian beam propagation equation.[26]

Data were acquired from photodiodes in combination with a gated boxcar integrator (SR200 series, Stanford Research Systems) while the sample was translated through the focus by a computer-controlled translation stage. The accuracy of the Z-scan measurement was probed by measuring the TPA cross-section of Rhodamine 6G (2.13×10^{-3} M in methanol) at a wavelength of 685 nm and the measured value (76.9 GM[27]) is consistent with values in the literature (~55 to 97 GM[28]). The TPA cross-section of each dye was measured in spectroscopic grade toluene in a 1 mm path-length fused quartz cuvette.

3. Results and discussion

In connection with the development of 3-dimensional optical data storage materials, we recently reported the TPA cross-section of chromophore **A2**,[6] a 1,4-bis-(α-cyano-4-(2-alkyloxystyryl))-2,5-dialkoxybenzene derivatized with methoxy and octadecyloxy groups in the central and peripheral positions, respectively (Fig. 1).[6,24] The nonlinear optical characteristics of this dye were explored, because its structure offers several features typically associated with a large σ, including extended

conjugation,[29] a large extent of symmetric charge transfer upon excitation,[13] and donor/acceptor functionalization.[12] The TPA cross-section of **A2**, determined using the open-aperture Z-scan method as a function of wavelength in the range of 625 to 725 nm, where the linear absorption is negligible, was found to reach a maximum of ~650 GM at 675 nm.[6] Using this data point, the T_m (154 °C), the solubility (1×10^{-3} M), the UV-Vis absorption maximum (λ_{abs} = 371 nm), and the PL emission maximum (λ_{em} = 507 nm) in $CHCl_3$ solution as starting points (Table 1), we explored systematic structural variations with the objective to create an OPV with maximum σ and solubility and minimal T_m. Compounds **A1**,[23] **A3**,[22] and **A4** with identical electronic structure, but different peripheral substituents, were synthesized *via* the Knoevenagel reaction of (4-alkyloxyphenyl) acetonitriles, which are readily accessible through alkylation of the parent (4-hydroxyphenyl)acetonitriles,[22–24] with 2,5-dimethoxyterephthalaldehyde (**A1**, **A3**) or 2,5-dioctyloxyterephthalaldehyde (**A4**). As expected, the UV-Vis absorption and PL emission spectra of these chromophores in $CHCl_3$ solution (Table 1, Fig. S2† and ref. 22–24) are essentially identical and match that of **A2** (Fig. 4). Fig. 2, which shows σ of selected dyes as a function of wavelength measured by an open-aperture Z-scan measurement, reveals that the TPA cross-sections of the series **A1–A4** are comparable, with a maximum of between ~630 and 858 GM at 675 nm (*i.e.*, within the commonly accepted error of ±15%).[30,31] We note that in these symmetric dyes, TPA will probe two-photon allowed Ag symmetry states rather than the one-photon allowed Bu states. Indeed, Z-scan measurements conducted at pump energies near half the one photon absorption maxima yielded negligible TPA signal. The common dispersion among these various chromophores is interesting and worthy of quantum chemical studies. The processability of these dyes, however, was found to vary considerably (Table 1). The T_m of **A1**, carrying four methoxy groups, is almost 250 °C. Substitution of the two peripheral methoxy against octadecyloxy groups (**A2**) led to a reduction of T_m by almost 100 °C, but proved to decrease the solubility in $CHCl_3$. The introduction of two peripheral ethylhexyloxy groups (**A3**) caused a similar reduction of T_m, but increased the solubility by an order of magnitude in comparison to **A1**. **A4**, featuring the sterically hindered ethylhexyloxy groups in the peripheral position and two octadecyloxy groups on the central benzene ring, displayed by far the best processability, with a melting temperature of 84 °C, *i.e.*, 55–70 °C lower than that of **A3** and **A2**, and a higher solubility than **A3**. This behavior is consistent with the large melting and dissolution entropies imparted by both substituent types, in particular the sterically demanding ethylhexyloxy groups.[32–34] Fig. 3 shows this by comparing differential scanning calorimetry (DSC) traces of the first heating of **A1**, **A3**, and **A4** (note that the small endothermic transition observed for **A3** at 137 °C is not seen in the second heating trace and appears to be related to polymorphs; also note that dye **A2** exhibits a solid to liquid crystalline transition below T_m).[24] Chromophores **B1** and **B2** are simple structural variations of the A-series and simply lack the two methoxy groups attached to the central benzene ring. Consistent with the lower degree of substitution, the solubility of these dyes is somewhat lower than that of the corresponding **A1** and **A3** and the melting temperatures are somewhat higher. The absorption and emission spectra of the B-dyes are blue-shifted and σ is considerably reduced (Table 1 and Fig. 4). These changes are consistent with a reduction of symmetric charge transfer brought about by the omission of the two donor groups.

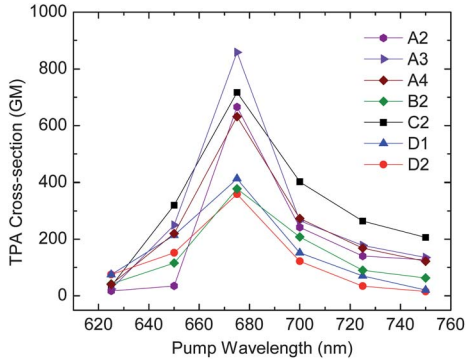

Fig. 2 TPA cross-section of OPV dyes investigated in this study as a function of wavelength measured by open-aperture Z-scan measurements (1 GM = 10^{-50} cm^4 s^{-1} $photon^{-1}$) in toluene.

In order to increase the extent of symmetric charge transfer, and therewith σ, **C1** and **C2**, carrying electron-withdrawing nitro groups in the peripheral positions, were investigated. Not

Table 1 Optical properties and isotropic melting temperatures of the dyes investigated in this study

Dye[a]	Abs λ_{max} in $CHCl_3$/nm	PL λ_{max} in $CHCl_3$/nm	PL λ_{max} of solid/nm	T_m/°C[b]	Solubility in $CHCl_3$ (M)	TPA cross-section in toluene, σ (GM)[d]	σ/N_{eff}[e]
A1	365, 436	513, 536	644	248	2×10^{-2}	—	—
A2	371, 437	507, 538	644	154	1×10^{-3}	666	26
A3	371, 440	508, 541	619	141	1×10^{-1}	858	33
A4	371, 434	511, 544	594	84	2×10^{-1}	632	24
B1	389	461, 486	550	279	9×10^{-3}	—	—
B2	397	464, 487	552	157	5×10^{-2}	378	15
C1	374	No PL	543	325	$\ll 4 \times 10^{-4}$[c]	—	—
C2	360, 458	553	618	191	8×10^{-3}	717	28
D1	346, 446	526	575	149	1×10^{-2}	359	14
D2	353, 442	531	584	113	5×10^{-3}	413	16

[a] Absorbance, emission, and thermal data for dyes **A1**,[23] **A2**,[24] **A3**,[22] and **B1**[23] were reproduced from earlier publications. [b] The isotropic melting temperature is listed here. Dyes **A2** and **B1** exhibit solid to liquid crystalline transitions below this temperature.[23,24] [c] **C1** was not dissolved at this concentration. [d] The TPA resonance for all dyes was between 650 and 700 nm. In the case of **A1**, **B1**, and **C1** the solubility in toluene was too low for an accurate determination of σ. [e] All molecules studied have an N_{eff} value (number of pi-electrons effectively involved in conjugation)[36] of 26.

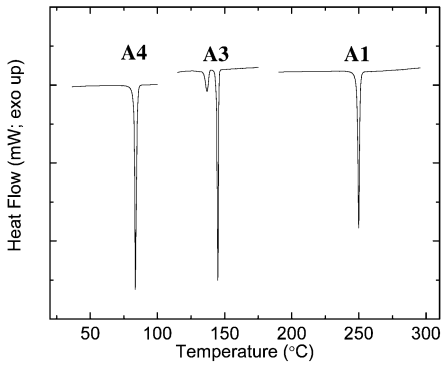

Fig. 3 Differential scanning calorimetry (DSC) traces (first heating, heating rate 10 °C min^{-1}) showing the melting transitions of dyes **A1**, **A3**, and **A4**.

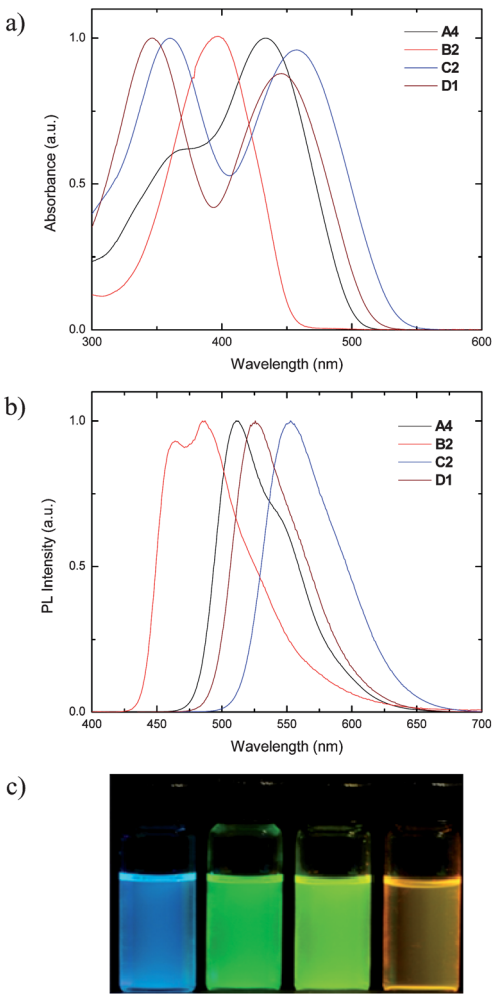

Fig. 4 (a) UV-Vis absorbance and (b) fluorescence spectra (excitation at 365 nm) of solutions of dyes **A4**, **B2**, **C2**, and **D1** in chloroform (*ca.* 2–5 × 10^{-5} M). (c) Digital images of solutions of dyes **B2**, **A4**, **D1**, and **C2** (left to right) in chloroform upon excitation at 365 nm.

surprisingly, **C1**, bare of any substituent on the central ring, showed the highest T_m and lowest solubility of all compounds investigated here, preventing any characterization in solution. The introduction of 3,7-dimethyloctyloxy groups (**C2**) had the expected effect on the processability, dropping T_m to below 200 °C and increasing the solubility by almost two orders of magnitude. The absorption spectrum shows a slight red-shift compared to the B-series on account of the strongly electron withdrawing nitro substituents. However, unlike dye **B1**, the fluorescence of **C1** was completely quenched, likely because the nitro groups stabilize the excited state *via* inductive effects.[35] The fluorescence intensity of **C2** is much higher than that of **C1**, presumably on account of an increased ICT, resulting in a smaller HOMO/LUMO gap. The σ of **C2** is among the highest measured here. Interestingly, however, it does not surpass the values of the A-series, which possesses weaker electron accepting functional groups (cyano), likely because it lacks the same compact D–π–A–π–D–π–A–π–D motif.

In the case of **D1** and **D2**, the peripheral 4-alkyloxyphenyl moieties were substituted with slightly less electron-rich 4-pyridinyl (**D1**) and 2-pyridinyl (**D2**) groups. By and large, the optical properties of these molecules are comparable to those of the A-series, although the TPA cross-section is somewhat lower (359 GM for **D1** and 413 GM for **D2**). The melting points of the dyes are at the low end of the spectrum (149 °C for **D1** and 113 °C for **D2**), and their solubility is high. This is clearly the result of the 3,7-dimethyloctyloxy groups, which induce large melting and dissolution entropies. The difference in melting points reflects the lower symmetry of **D2** in comparison to **D1**.

Several CN′′-OPVs, including **A1** and **A2**, have previously been shown to form excimers upon aggregation so that solutions and solid materials display rather different fluorescence spectra. This "chameleon behavior" is the result of intramolecular interactions and in the case of static (as opposed to dynamic) complexes strongly depends on the molecular packing.[21e] The previously reported dyes of the A-series (**A1–A3**) display green emission in $CHCl_3$ solution, with λ_{em} = 507–511 nm (Table 1). Their solid-state emission is orange-red, with identical λ_{em} = 644 nm for **A1**[23] and **A2**.[24] The solid-state emission of **A3**[22] is blue-shifted by 25 nm compared to **A1** and **A2**, presumably due to a less compact crystal structure by the bulky ethylhexylgroups. In fact, the crystal structure for **A1** shows a strong twisting of the molecular backbone, a likely effect of accommodating the strong intermolecular charge transfer interactions.[21e] The twisting is much less pronounced in **A3**; its crystal structure reveals a rather planar molecule, suggesting that the bulky substituents reduce the intermolecular charge transfer due to less effective orbital overlap between adjacent molecules (Fig. S3†).

The absorption and fluorescence spectra of the new dyes **A4**, **B2**, **C2**, and **D1**, both in chloroform and solid state, are shown in Fig. 5, together with pictures of the corresponding samples. The quantum yield of **A4** and **B2**, which serve as prototype for the respective series, was for both dyes determined to be 0.47 in toluene solution. As can be seen, the emission spectra of solution and solid state (also evident from the digital images shown in Fig. 5) of all dyes display pronounced differences, and in particular **A4** and **B2** show featureless broadened solid-state spectra that are indicative of excimer formation.[23] Aggregation experiments in mixed solvent systems (MeOH/$CHCl_3$ for **B2**, **C2** and THF/H_2O for **A3**; Fig. S4†) have not revealed any changes in the absorption spectra that are indicative of ground-state interactions. This observation is in line with the previous findings for

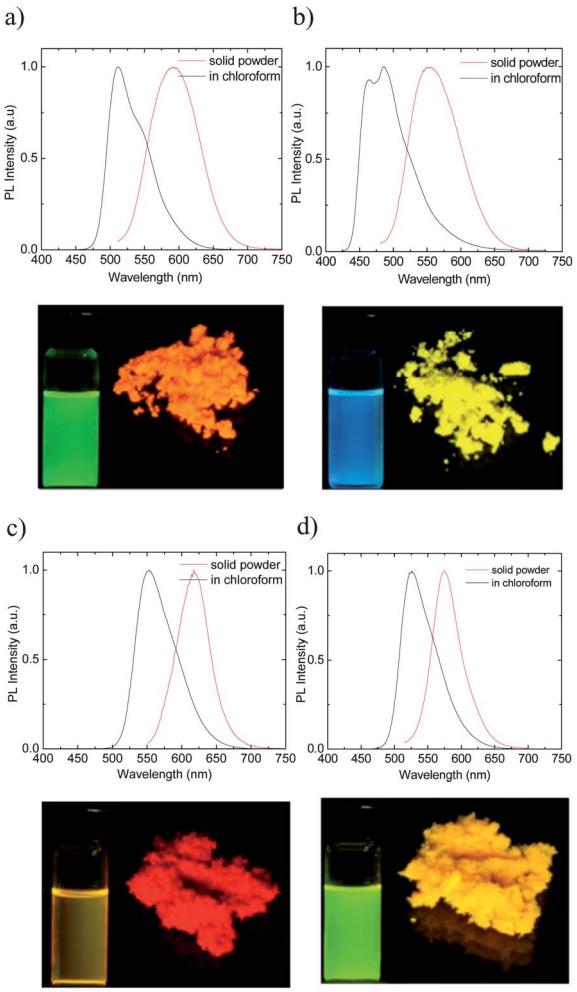

Fig. 5 Fluorescence spectra (excitation at the wavelength of absorbance maximum) and digital images (under excitation at 365 nm) of (a) **A4**, (b) **B2**, (c) **C2**, and (d) **D1** in chloroform and as a solid powder.

A and B series dyes, with the exception of **A2**, which displays considerable charge-transfer interactions in the solid state.[24]

A4 continues the trend set by **A3** vis a vis **A1** and **A2** in that functionalization with bulky substituents (*i.e.* the combination of octyloxy groups attached to the aromatic core and 2-ethylhexyloxy groups in the peripheral positions) blue-shifts the solid state spectra by another 25 nm in comparison to **A3**. The emission characteristics of **B2** are identical to those of **B1**. In view of the hypsochromic shift observed between **A3** and **A1** (*vide supra*) and the fact that dyes of the B-series with long linear peripheral alkyloxy groups (dodecyloxy and octadecyloxy) show blue monomer emission,[21e] this finding is quite intriguing, as a low-melting, yellow-blue color-changing excimer-forming cyano-OPV has so far not been available. As was shown previously, the formation of ground-state excimers in cyano-OPVs is usually the result of crystal structures, in which adjacent molecules are shifted with respect to one another so that the electron-poor cyano-group overlaps with the electron-donating central ring of its neighbor.[21e] In the case of B-series derivatives with long linear peripheral alkyloxy groups, interactions between the latter prevail over π–π interactions, imparting crystal structures that do not lend themselves to excimer emission.[21e] In this context, the 2-ethylhexyloxy tails appear to be ideal, as they impart the new **B2** with low melting temperature and high solubility without providing strong interactions that have a governing influence on the dye's solid state structure.

C2 displays a deep red solid-state emission (Table 1 and Fig. 5c) centered around 618 nm, which is shifted by 65 nm compared to the emission maximum in solution. The contrast between solution and solid state for **C2** is smaller than that of any dye in the A or B-series, which is perhaps a result of the bulky 3,7-dimethyloctyloxy groups, which prevent compact crystal packing, much in the same way as was suggested for the A and B-series based upon the trend of higher energy emission for increasing bulkiness seen for those dyes.

Molecules **D1** and **D2** are almost identical in structure and their spectra are indeed very similar. The D series also has bulky 3,7-dimethyloctyloxy groups much like the C-series which can frustrate excimer formation. Furthermore, the weakly electron donating nitrogen accounts for much less ICT as the nitro substituents in the C-series or the alkyloxy substituents in the A or B-series, so it is not surprising that the D-series exhibits the smallest contrast between emission of solution and solid state (49 and 53 nm for **D1** and **D2**, respectively). Indeed the digital images in Fig. 5 show the least impressive contrast between emission of solution and solid state.

The excimer-forming propensity of the new chromophores is useful for the design of stimuli-responsive, color-changing fluorescent polymers, which are produced by incorporating small amounts of excimer-forming dyes into a host polymer of interest.[21] The general approach relies on the stimulus-driven self-assembly (*e.g.* upon exposure to heat, chemicals) or dissociation (*e.g.* upon mechanical deformation, exposure to light) of nanoscale aggregates of these dyes in a host polymer, which results in a pronounced change in the fluorescence color. Some representatives of the **A** and **B** series have already proven to be very useful in this context. They have been shown to be stable under melt-processing conditions at temperatures of over 250 °C in a variety of host polymers, which bodes well for the exploitation of the new dyes in such a context.

4. Conclusions

In conclusion, we have measured large TPA cross-sections in the range of 400–850 GM for several CN″-OPVs, a class of molecules whose optical nonlinearities have previously little been studied. The functionalization with bulky alkyloxy substituents has afforded derivatives that display a melting point as low as 84 °C and a solubility in chloroform as high as 2×10^{-1} M while exhibiting a σ of ~630 GM. These CN″-OPVs have the propensity to form excimers and exhibit a wide array of absorption/emission colors, which are dependent on the functionalization of the OPV motif with electron accepting and donation groups.

The combination of significant optical nonlinearity, low melt-processing temperature, high thermal stability, and the propensity for excimer-formation makes the new CN″-OPVs interesting candidates for a range of applications, in particular optical data storage systems that function on the basis of TPA-induced switching of the aggregation state and fluorescence color.[6] The

availability of such dyes which cover a range of emission colors makes the design of complex systems with a multitude of switching states for each voxel possible.

Acknowledgements

This work is based on research supported by the US National Science Foundation (NSF) under grant no DMR-0602767 (Materials World Network) and DMR-0423914 (Center for Layered Polymer Systems at Case Western Reserve University). We also acknowledge financial support from the Adolphe Merkle Foundation and thank P.W. Nolte, D. Pergande, M. Geuss, D. Langhe, M. Steinhart, K. Busch, and R.B. Wehrspohn for stimulating discussions. We are grateful to the research group of John D. Protasiewicz for help with the determination of crystal structures.

References

1 M. Pawlicki, H. A. Collins, R. G. Denning and H. L. Anderson, *Angew. Chem., Int. Ed.*, 2009, **48**, 3244.
2 S. Klein, A. Barsella, H. Leblond, H. Bulou, A. Fort, C. Andraud, G. Lemercier, J. C. Mulatier and K. Dorkenoo, *Appl. Phys. Lett.*, 2005, **86**, 211118.
3 D. D. Yavuz, *Phys. Rev. A: At., Mol., Opt. Phys.*, 2006, **74**, 53804.
4 D. Fichou, V. Dumarcher and J. M. Nunzi, *Opt. Mater.*, 1999, **12**, 255.
5 V. Mizrahi, K. W. DeLong, G. I. Stegeman, M. A. Saifi and M. J. Andrejco, *Opt. Lett.*, 1989, **14**, 1140.
6 J. Lott, C. Ryan, B. Valle, J. R. Johnson, III, D. A. Schiraldi, J. Shan, K. D. Singer and C. Weder, *Adv. Mater.*, 2011, **23**, 2425.
7 W. Denk, J. H. Strickler and W. W. Webb, *Science*, 1990, **248**, 73.
8 L. Beverina, M. Crippa, M. Landenna, R. Ruffo, P. Salice, F. Silvestri, S. Versari, A. Villa, L. Ciaffoni, E. Collini, C. Ferrante, S. Bradamente, C. M. Mari, R. Bozio and G. Pagani, *J. Am. Chem. Soc.*, 2008, **130**, 1894.
9 S. Kawata, H. B. Sun, T. Tanaka and K. Takada, *Nature*, 2001, **412**, 697.
10 F. Lincker, P. Masson, J. F. Nicoud, P. Didier, L. Guidoni and J. Y. Bigot, *J. Nonlinear Opt. Phys. Mater.*, 2005, **14**, 319.
11 A. Bhaskar, R. Guda, M. M. Haley and T. Goodson, III, *J. Am. Chem. Soc.*, 2006, **128**, 13972.
12 M. Albota, D. Beljonne, J. L. Brédas, J. E. Ehrlich, J. Y. Fu, A. A. Heikal, S. E. Hess, T. Kogej, M. D. Levin, S. R. Marder, D. McCord-Maughon, J. W. Perry, H. Röckel, M. Rumi, G. Subramaniam, W. W. Webb, X. L. Wu and C. Xu, *Science*, 1998, **281**, 1653.
13 M. Rumi, J. E. Ehrlich, A. A. Heikal, J. W. Perry, S. Barlow, Z. Hu, D. McCord-Maughon, T. C. Parker, H. Röckel, S. Thayumanavan, S. R. Marder, D. Beljonne and J. L. Brédas, *J. Am. Chem. Soc.*, 2000, **122**, 9500.
14 P. W. Nolte, D. Pergrande, S. L. Schweizer, M. Geuss, R. Salzer, B. T. Makowski, M. Steinhart, P. Mack, D. Herrmann, K. Busch, C. Weder and R. B. Wehrspohn, *Adv. Mater.*, 2010, **22**, 4731.
15 H. Song, K. D. Singer, J. Lott, Y. Wu, J. Zhou, J. H. Andrews, E. Baer, A. Hiltner and C. Weder, *J. Mater. Chem.*, 2009, **19**, 7520.
16 H. Y. Woo, B. Liu, B. Kohler, D. Korystov, A. Mikhailovsky and G. C. Bazan, *J. Am. Chem. Soc.*, 2005, **127**, 14721.
17 H. M. Kim and B. R. Cho, *Chem. Commun.*, 2009, 153.
18 S. J. K. Pond, M. Rumi, M. D. Levin, T. C. Parker, D. Beljonne, M. W. Day, J. L. Brédas, S. Marder and J. W. Perry, *J. Phys. Chem. A*, 2002, **106**, 11470.
19 P. F. van Hutten, V. V. Krasnikov, H. J. Brouwer and G. Hadziioannou, *Chem. Phys.*, 1999, **241**, 139.
20 B. Wang, Y. Wang, J. Hua, Y. Jiang, J. Huang, S. Qian and H. Tian, *Chem. Eur. J.*, 2011, **17**, 2647.
21 See for example: (*a*) B. R. Crenshaw and C. Weder, *Chem. Mater.*, 2003, **15**, 4717; (*b*) J. Kunzelman, B. R. Crenshaw, M. Kinami and C. Weder, *Macromol. Rapid Commun.*, 2006, **27**, 1981; (*c*) J. Kunzelman, B. R. Crenshaw and C. Weder, *J. Mater. Chem.*, 2007, **17**, 2989; (*d*) B. R. Crenshaw, M. Burnworth, D. Khariwala, A. Hiltner, P. T. Mather, R. Simha and C. Weder, *Macromolecules*, 2007, **40**, 2400; (*e*) J. Kunzelman, M. Kinami, B. R. Crenshaw, J. D. Protasiewicz and C. Weder, *Adv. Mater.*, 2008, **20**, 119; (*f*) J. Kunzelman, C. Chung, P. T. Mather and C. Weder, *J. Mater. Chem.*, 2008, **18**, 1082; (*g*) J. Kunzelman, M. Gupta, B. R. Crenshaw, D. A. Schiraldi and C. Weder, *Macromol. Mater. Eng.*, 2009, **294**, 244; (*h*) L. Tang, J. Whalen, G. Schutte and C. Weder, *ACS Appl. Mater. Interfaces*, 2009, **2**, 688; (*i*) C. Weder, *Chimia*, 2009, **63**, 758; (*j*) J. Lott and C. Weder, *Macromol. Chem. Phys.*, 2010, **211**, 28; (*k*) B. Makowski, J. Kunzelman and C. Weder, *Handbook of Stimuli-Responsive Materials*, Wiley-VCH, Weinheim, 2011.
22 B. R. Crenshaw and C. Weder, *Chem. Mater.*, 2003, **15**, 4717.
23 C. Löwe and C. Weder, *Synthesis*, 2002, **9**, 1185.
24 M. Kinami, B. R. Crenshaw and C. Weder, *Chem. Mater.*, 2006, **18**, 946.
25 M. Sheik-Bahae, A. Said, T. Wei, D. Hagan and E. Van Stryland, *IEEE J. Quantum Electron.*, 1990, **26**, 760.
26 P. Milonni and J. Eberly, Laser Resonators, in *Lasers*, John Wiley & Sons, New York, 1988, p. 486.
27 1 GM $\equiv$ 1 $\times$ 10–50 cm^4 s $photon^{-1}$.
28 N. Makarov, M. Drobizhev and A. Reband, *Opt. Express*, 2008, **16**, 4029.
29 M. Johnsen, M. J. Paterson, J. Arnbjerg, O. Christiansen, C. B. Nielsen, M. Jørgensen and P. R. Ogilby, *Phys. Chem. Chem. Phys.*, 2008, **10**, 1177.
30 Z. Zeng, Z. Guan, Q. H. Xu and J. Wu, *Chem.–Eur. J.*, 2011, **17**, 3837.
31 T. C. Lin, G. S. He, P. N. Prasad and L. S. Tan, *J. Mater. Chem.*, 2004, **14**, 982.
32 A. R. A. Palmans, M. Eglin, A. Montali, C. Weder and P. Smith, *Chem. Mater.*, 2000, **12**, 472.
33 A. R. A. Palmans, P. Smith and C. Weder, *Macromolecules*, 1999, **32**, 4677.
34 C. Weder and M. S. Wrighton, *Macromolecules*, 1996, **29**, 5157.
35 C. Munkholm, D. R. Parkinson and D. R. Walt, *J. Am. Chem. Soc.*, 1990, **112**, 2608.
36 M. G. Kuzyk, *J. Chem. Phys.*, 2003, **119**, 8327.

